Pis'ma v ZhETF, vol. 100, iss. 1, pp. 30 – 33

Anomalous spin relaxation and quantum criticality in $Mn_{1-x}Fe_xSi$ solid solutions[1)]

S. V. Demishev[+*2)], *A. N. Samarin*[+*], *V. V. Glushkov*[+*], *M. I. Gilmanov*[+*], *I. I. Lobanova*[+*], *N. A. Samarin*[+], *A. V. Semeno*[+], *N. E. Sluchanko*[+], *N. M. Chubova*[×], *V. A. Dyadkin*[×], *S. V. Grigoriev*[×]

[+]*Prokhorov General Physics Institute of the RAS, 119991 Moscow, Russia*

[*]*Moscow Institute of Physics and Technology, 141700 Dolgoprudny, Russia*

[×]*Konstantinov St.Petersburg Nuclear Physics Institute, 188300 Gatchina, Russia*

Submitted 27 May 2014

We report results of the high frequency (60 GHz) electron spin resonance (ESR) study of the quantum critical metallic system $Mn_{1-x}Fe_xSi$. The ESR is observed for the first time in the concentration range $0 < x < 0.24$ at temperatures up to 50 K. The application of the original experimental technique allowed carrying out line shape analysis and finding full set of spectroscopic parameters, including oscillating magnetization, line width and g factor. The strongest effect of iron doping consists in influence on the ESR line width and spin relaxation is marked by both violation of the classical Korringa-type relaxation and scaling behavior. Additionally, the non-Fermi-liquid effects in the temperature dependence of the ESR line width, which may be quantitatively described in the theory of Wölfle and Abrahams, are observed at quantum critical points $x^* \sim 0.11$ and $x_c \sim 0.24$.

DOI: 10.7868/S0370274X14130062

Since the pioneering work [1], which established the modern history of the study of the magnetic resonance in strongly correlated metals (SCM), the importance of the ferromagnetic (FM) correlations in the genesis of the electron spin resonance (ESR) in very different systems like $YbRh_2Si_2$ [1, 2], CeB_6 [3–5] or CeRuPO [6] is well understood. Interesting, that in some cases the proximity to FM quantum critical (QC) point and related FM fluctuations was driving the ESR physical picture [1, 2, 6] and hence the problem of the relation between quantum criticality and electron spin resonance appears on the agenda. For studying of this issue, the spiral magnets $Mn_{1-x}Fe_xSi$ may be considered as prospective objects possessing both FM interactions [7] and $T-x$ magnetic phase diagram with two QC points located at $x^* \sim 0.11$ and $x_c \sim 0.24$ [8], which divide the concentration axis at $T = 0$ into the regions of stability of the spiral phase with long-range magnetic order ($0 < x < x^*$) and short range magnetic order ($x^* < x < x_c$) [8]. The diapason $x > x_c$ is characterized by onset of the Griffiths anomaly of the magnetic susceptibility [8]. Additional interest in this case arises from the fact that most of ESR measurements in SCMs were carried out for the f-electron materials, whereas $Mn_{1-x}Fe_xSi$ system is an example of d-electron magnet. At present there are only few published works on magnetic resonance in MnSi [9–11] and dynamic magnetic properties of substitutional solid solutions $Mn_{1-x}Fe_xSi$ with $x > 0$ have never been reported.

We have studied single crystals of $Mn_{1-x}Fe_xSi$ system in the diapason of iron concentration $x < 0.3$. The quality of samples grown by Czochralski and Bridgeman methods was controlled by X-ray and neutron scattering diffraction; the real chemical composition was determined from EPMA experiments. In addition to high frequency (60 GHz) ESR experiments, the resistivity, magnetoresistance and magnetization have been measured in the temperature range 1.8–300 K in magnetic field up to 8 T. The magnetic field was aligned along [110] direction. Analysis of the physical characteristic obtained shows that the studied samples are either identical or very close to those known from the literature [7–12].

Before describing the results of the ESR experiment and data analysis it is important to consider the magnetic phase diagram of $Mn_{1-x}Fe_xSi$. It is known, that in a finite and relatively strong magnetic field corresponding to high-frequency ESR measurements the magnetic phase diagram of MnSi acquires relatively simple character and consists of the paramagnetic (P) and ferromagnetic (spin-polarized, SP) phases [10, 11]. The study

[1)]See Supplemental material for this paper on JETP Letters suite: www.jetpletters.ac.ru.

[2)]e-mail: demis@lt.gpi.ru

carried out in [11] revealed that the best way for a correct finding of the phase boundaries in this case consists in use of the magnetoresistance rather than magnetization or magnetic susceptibility data. The reason for that is the domination of the Yosida mechanism of the magnetic scattering [13], which leads to universal proportionality of the magnetoresistance to magnetization square $\Delta\rho/\rho \sim -M^2$ in the paramagnetic phase [11, 13]. When lowering the temperature leads to a transition into the SP phase the above relation breaks due to the switching off the channel of the magnetic scattering corresponding to the opposite spins orientations and, as a result, the minimum of the negative magnetoresistance temperature dependence $\Delta\rho/\rho = f(B = \text{const}, T)$ located exactly at P–SP-phase boundary is formed [11].

It is found that the aforementioned behavior established for pure MnSi also holds in the studied $Mn_{1-x}Fe_xSi$ solid solutions and the same method can be applied for determination of the $T-x$ magnetic phase diagram (the necessary details are provided in the supplementary materials [14]). The result for the magnetic field corresponding to the 60 GHz ESR line position $B = B_{res} \sim 2.2$ T is shown in Fig. 1. It worth noting that in the range $0.19 \le x \le 0.24$ the minimum on the $\Delta\rho/\rho = f(B = \text{const}, T)$ is not observed, and for the corresponding samples we suppose that the transition temperature into SP phase, T_{SP}, is close to zero. The obtained magnetic phase diagram is somewhat different from that reported in [8] for $B = 0$. Firstly, QC point at $x^* \sim 0.11$, if it still exists, is hidden inside SP phase. Secondly, the concentration region $x^* < x < x_c$, where the phase with short-range magnetic order was observed in [8], becomes partly substituted by the SP phase. Therefore, the possible relation between quantum criticality and ESR in $Mn_{1-x}Fe_xSi$ may be quite complicated.

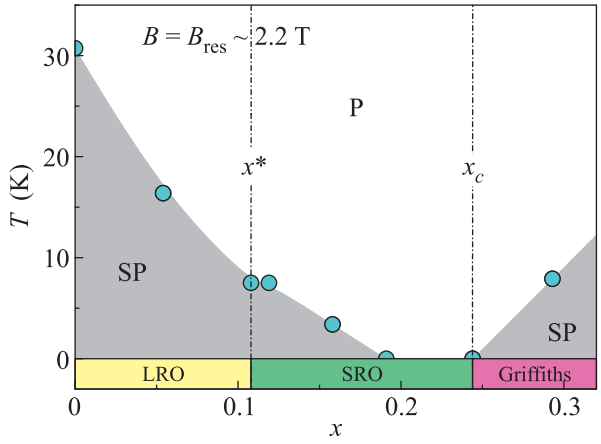

Fig. 1. The $T-x$ magnetic phase diagram of $Mn_{1-x}Fe_xSi$ in the resonant field $B_{res} \sim 2.2$ T and quantum phase transitions expected in the case $B = 0$ according to Ref. [8]

For studying of the ESR in $Mn_{1-x}Fe_xSi$ we have used original technique, which includes special geometry of the cavity measurements and allows absolute calibration of the cavity absorption caused by the sample in units of the magnetic permeability μ [4, 10, 11]. For that purpose standard microwave measurements should be added by magnetoresistance data for the model-free subtraction of the base line and magnetization data for the correct accounting of the local field acting on the oscillating spins. Fitting of the experimental data in the absolute units with the help of known models for dynamic susceptibilities allows finding the full set of ESR parameters, including oscillating magnetization M_0, g factor, and the line width W [4, 10, 11]. Earlier this technique was successfully applied to the case of pure MnSi [10, 11].

Examples of absolutely calibrated ESR spectra evolution with temperature and iron concentration in $Mn_{1-x}Fe_xSi$ are presented in Figs. 2 and 3 respectively. In all cases $\mu(B = 0) = 1$ and data in these figures are

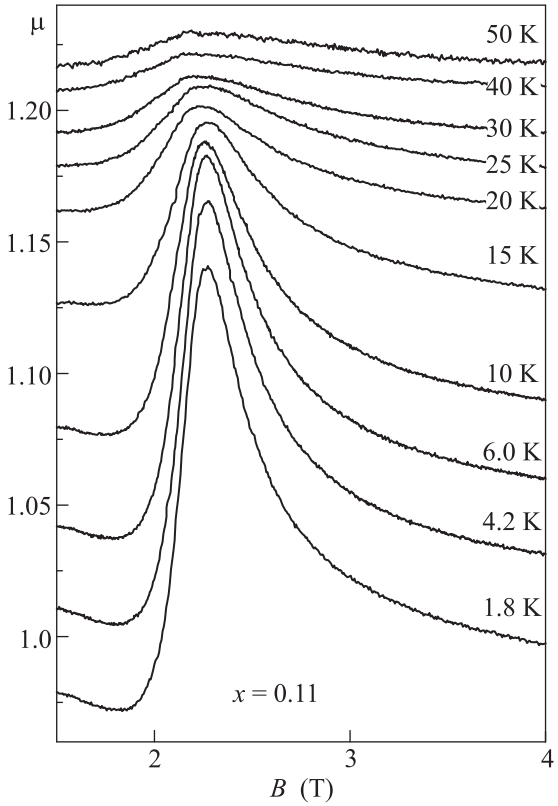

Fig. 2. Temperature evolution of the ESR spectra of the sample with $x = 0.11$

shifted for clarity. Additionally a scale factor is applied to each $\mu(B)$ curve in Fig. 3. In general case, magnetic resonance can be observed in both paramagnetic and

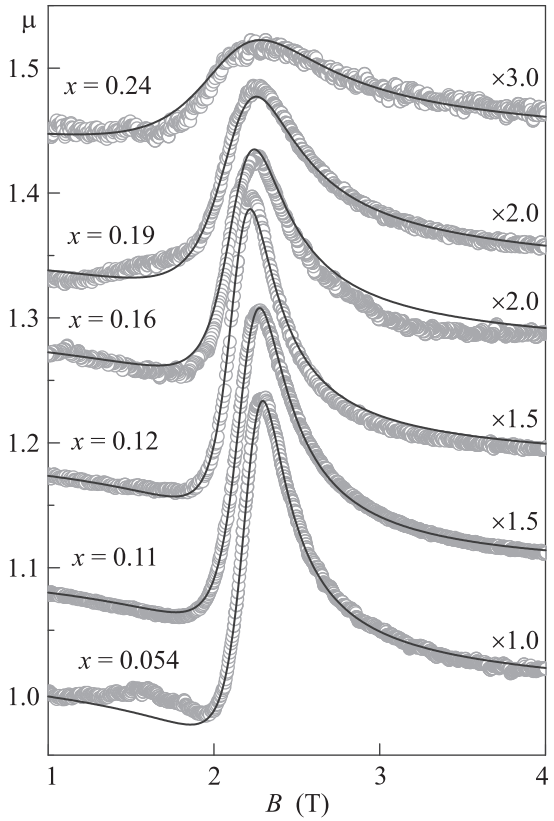

Fig. 3. The ESR spectra for $Mn_{1-x}Fe_xSi$ samples with various x at $T = 4.2$ K. The corresponding scale factors are shown at the right of each curve. Points correspond to the experiment and the lines denote results of model approximation.

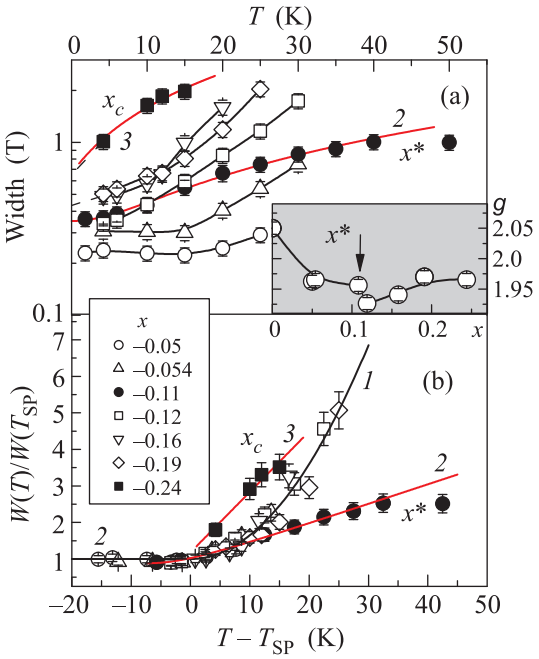

Fig. 4. Temperature dependences of the line width (a) and scaling behavior (b) in $Mn_{1-x}Fe_xSi$. Line *1* in panel b is the fitting by the scaling function, the lines *2* and *3* corresponds to approximation in the NFL model (see text for details). The inset shows concentration dependence of the g factor

spin-polarized phases. It is visible that both increase in temperature and x results in broadening of the ESR line and simultaneous decrease of its amplitude. The temperature domain for the ESR observation shrinks with the iron concentration and above critical concentration $x_c \sim 0.24$ no magnetic resonance is detected. The experimental ESR line shape can be well reproduced in the model of oscillating localized magnetic moments (see solid lines in Fig. 3). Fitting with the help of three model parameters, M_0, g, and W, gives that oscillating magnetization M_0 is equal to the total static magnetization M for all samples studied at all temperatures where ESR can be observed. This result is in agreement with the data reported previously [10, 11] for pure MnSi. For that reason in further calculations, we have fixed parameter $M_0 = M$, which allowed to achieve better accuracy of the g factor and line width determination.

It is found that in $Mn_{1-x}Fe_xSi$ system the g factor is not dependent on temperature. The increase of iron concentration results in a decrease of the $g(x)$ by $\approx 5\,\%$ in the diapason $0 < x < x^*$ followed by a kink at characteristic concentration x^* (inset in Fig. 4a). Further enhancement of x leads to a gradual increase of the g factor up to the limiting concentration x_c (inset in Fig. 4a). The data obtained on the ESR line width are summarized in Fig. 4a. The maximal temperature, for which the line width $W(x,T)$ was calculated, depended on the line broadening as well as on the single crystal size available for the ESR measurements. Taking this into account, the observed $W(x,T)$ variation in $Mn_{1-x}Fe_xSi$ may reach at least the order of magnitude (Fig. 4a), and hence the strongest effect of iron doping consists in influence on the ESR line width and spin relaxation.

Interesting, that for the majority of compositions, the $W(x,T)$ data can be reduced to the universal scaling dependence $W(x,T)/W(T_{SP}) = f(T - T_{SP})$ (Fig. 4b). The value $W(T_{SP})$ was determined either by interpolation or extrapolation of the experimental $W(T)$ dependence either to the $T_{SP}(x) \neq 0$ point, or to $T_{SP} = 0$ for $0.19 \leq x \leq 0.24$ (see Fig. 1). It follows from Fig. 4b that the universal behavior holds for all iron concentrations, except those corresponding to the QC points $x^* \sim 0.11$ and $x_c \sim 0.24$. The scaling function $f(z)$ acquires a relatively simple form $f(z < 0) \approx 1$ and $f(z > 0) \approx 1 + a_0 z^2$, where the coefficient a_0 equals $6.5 \cdot 10^{-3}\,\mathrm{K}^{-2}$ (solid line *1* in Fig. 4b).

The discovered scaling behavior constitutes anomaly of the first kind in the spin relaxation of $Mn_{1-x}Fe_xSi$.

Indeed, the classical explanation of the line widths observed in the ESR of magnetic ions in metals is based on Korringa mechanism [15], which means that temperature dependent part of the line width $\Delta W(T)$ should be proportional to inversed spin susceptibility, $\Delta W(T) \sim 1/\chi(T)$. Some theoretical works suggest that the same description of the relaxation rate is possible in SCM, i.e. in the case of the magneto-optical response of the strongly correlated matrix of magnetic ions [5]. Assuming validity of Curie–Weiss law in $Mn_{1-x}Fe_xSi$ it is natural to expect the dependence $\Delta W(T) \sim 1/\chi(T) \sim (T - T_{SP})$, whereas experiment gives $\Delta W(T) \sim (T - T_{SP})^2$ (Fig. 4b).

In addition the violation of Korringa relaxation mechanism, there is an anomaly of the second kind, namely the departures from the universal behavior exactly at characteristic concentrations $x^* \sim 0.11$ and $x_c \sim 0.24$ (Fig. 4b), which are supposed to correspond to quantum phase transitions (see [8] and Fig. 1). This observation suggests that spin relaxation along the lines $x = x^*$ and $x = x_c$ is different from the rest of the $T-x$ magnetic phase diagram and related $W(T)$ dependences appear more weak (Fig. 4). The considered anomaly may be qualitatively explained by the theory of the ESR in SCM developed by Wölfle and Abrahams [16]. According to [16] in the Fermi-liquid (FL) regime $\Delta W(T) \sim T^2$, whereas in the non-Fermi-liquid (NFL) regime $\Delta W(T) \sim T$, and hence the anomaly of the second kind in $Mn_{1-x}Fe_xSi$ may be explained by the onset of NFL regime in the proximity of the quantum critical points. Taking the temperature dependent contribution to the line width in the form obtained in [16] it is possible to come to the model expression $W(T) = AT \arctan(T/T_x) + W_0$, where T_x denotes an energy scale for a crossover between FL ($T \ll T_x$) and NFL ($T \gg T_x$) cases. The above equation provides reasonable approximation for the experimental $W(T)$ curves for the samples with $x = 0.11$, and $x = 0.24$ assuming $T_x \sim 11$ K ($x = x^*$, lines *2* in Figs. 4a and b) and $T_x \sim 0$ ($x = x_c$, lines *3* in Figs. 4a and b). In agreement with the magnetic phase diagram (Fig. 1) it is possible to conclude that in both cases T_x is about transition temperature T_{SP}.

In conclusion, we have shown that spin relaxation in $Mn_{1-x}Fe_xSi$ solid solutions is very unusual and complicated and may involve two different mechanisms, one of which is responsible for violation of Korringa-type relaxation and gives the universal scaling behavior. Another mechanism is likely connected with the NFL effects [15] and develops at QC points $x^* \sim 0.11$ and $x_c \sim 0.24$, which presence has been suggested in [8]. Analysis of the ESR characteristics supports the real existence of the underlying QC point x^* which sometimes become a subject of debates (see [8, 12] and the references cited therein). Although this QC point is hidden inside the spin-polarized phase, it gives rise to specific spin relaxation even in the paramagnetic phase. We wish to emphasize that it is generally believed that underlying QC point in $Mn_{1-x}Fe_xSi$ cannot produce observable anomalies at finite temperatures [12]. Nevertheless, the current level of development of the ESR theory in SCM [2, 5, 15, 16] does not allow complete quantitative description of obtained experimental results, which demands further theoretical study of the relation between ESR and quantum critical phenomena in strongly correlated metals.

This work was supported by Programme of Russian Academy of Sciences "Strongly correlated electrons" and by RFBR grant # 13-02-00160.

1. J. Sichelschmidt, V. A. Ivanshin, J. Ferstl, C. Geibel, and F. Steglich, Phys. Rev. Lett. **91**, 156401 (2003).
2. E. Abrahams and P. Wölfle, Phys. Rev. B **78**, 104423 (2008).
3. S. V. Demishev, A. V. Semeno, Yu. B. Paderno, N. Yu. Shitsevalova, and N. E. Sluchanko, Phys. Stat. Sol. (b) **242**, R27 (2005).
4. S. V. Demishev, A. V. Semeno, A. V. Bogach, N. A. Samarin, T. V. Ishchenko, V. B. Filipov, N. Yu. Shitsevalova, and N. E. Sluchanko, Phys. Rev. B **80**, 245106 (2009).
5. P. Schlottmann, Phys. Rev. B **86**, 075135 (2012).
6. C. Krellner, T. Förster, H. Jeevan, C. Geibel, and J. Sichelschmidt, Phys. Rev. Lett. **100**, 066401 (2008).
7. S. V. Grigoriev, V. A. Dyadkin, E. V. Moskvin, D. Lamago, Th. Wolf, H. Eckerlebe, and S. V. Maleyev, Phys. Rev. B **79**, 144417 (2009).
8. S. V. Demishev, I. I. Lobanova, V. V. Glushkov, T. V. Ischenko, N. E. Sluchanko, V. A. Dyadkin, N. M. Potapova, and S. V. Grigoriev, JETP Lett, **98**, 829 (2013).
9. M. Date, K. Okuda, and K. Kadowaki, J. Phys. Soc. Jpn. **42**, 1555 (1977).
10. S. V. Demishev, A. V. Semeno, A. V. Bogach, V. V. Glushkov, N. E. Sluchanko, N. A. Samarin, and A. L. Chernobrovkin, JETP Lett. **93**, 213 (2011).
11. S. V. Demishev, V. V. Glushkov, I. I. Lobanova, M. A. Anisimov, V. Yu. Ivanov, T. V. Ishchenko, M. S. Karasev, N. A. Samarin, N. E. Sluchanko, V. M. Zimin, and A. V. Semeno, Phys. Rev. B **85**, 045131 (2012).
12. A. Bauer, A. Neubauer, C. Franz, W. Münzer, M. Garst, and C. Pfleiderer, Phys. Rev. B **82**, 064404 (2010).
13. K. Yosida, Phys. Rev. **107**, 396 (1957).
14. See Supplemental Material at [URL to be inserted by publisher].
15. S. E. Barnes, Adv. Phys. **30**, 801 (1981).
16. P. Wölfle and E. Abrahams, Phys. Rev. B **80**, 235112 (2009).